Absence of magnetic long-range order in Y_2CrSbO_7: Bond-disorder-induced magnetic frustration in a ferromagnetic pyrochlore

L. Shen,[1] C. Greaves,[2] R. Riyat,[1] T. C. Hansen,[3] and E. Blackburn[1]
[1]*School of Physics and Astronomy, University of Birmingham, Birmingham B15 2TT, United Kingdom*
[2]*School of Chemistry, University of Birmingham, Birmingham B15 2TT, United Kingdom*
[3]*Institut Laue-Langevin, BP 156, 38042 Grenoble Cedex 9, France*
(Received 27 February 2017; revised manuscript received 10 July 2017; published 28 September 2017)

The consequences of random nonmagnetic-ion dilution for the pyrochlore family $Y_2(M_{1-x}N_x)_2O_7$ (M = magnetic ion, N = nonmagnetic ion) have been investigated. As a first step, we experimentally examine the magnetic properties of Y_2CrSbO_7 ($x = 0.5$), in which the magnetic sites (Cr^{3+}) are percolative. Although the effective Cr-Cr spin exchange is ferromagnetic, as evidenced by a positive Curie-Weiss temperature, $\Theta_{CW} \simeq 19.5$ K, our high-resolution neutron powder diffraction measurements detect no sign of magnetic long-range order down to 2 K. In order to understand our observations, we construct a lattice model to numerically study the bond disorder introduced by the ionic size mismatch between M and N, which reveals that the bond disorder percolates at $x_b \simeq 0.23$, explaining the absence of magnetic long-range order. This model could be applied to a series of frustrated magnets with a pyrochlore sublattice, for example, the spinel compound $Zn(Cr_{1-x}Ga_x)_2O_4$, wherein a Néel to spin glass phase transition occurs between $x = 0.2$ and 0.25 [Lee *et al.*, Phys. Rev. B **77**, 014405 (2008)]. Our study stresses the non-negligible role of bond disorder on magnetic frustration, even in ferromagnets.

DOI: 10.1103/PhysRevB.96.094438

I. INTRODUCTION

Magnetic frustration, which often leads to interesting spin structures, refers to systems where the total free energy cannot be minimized by optimizing the interaction energy between each pair of spins [1]. Magnetic interactions can be frustrated by geometry. For example, magnetic long-range order is prohibited for the Heisenberg antiferromagnet on a triangular (or tetrahedral) lattice [2]. The corresponding magnetic ground state, named spin liquid, is highly degenerate [3–5]. In addition to geometry, the competition between different types of magnetic interactions can also lead to magnetic frustration. The Ising rare-earth pyrochlores $R_2Ti_2O_7$ (R = Ho, Dy), in which the R sublattice forms a corner-sharing tetrahedral network, develop a novel two-in/two-out spin ice structure due to the competing exchange and dipole-dipole interactions [2,6,7]. Strikingly, the excited quasiparticles of a spin ice are found to resemble the behavior of magnetic monopoles [8,9].

The effect of disorder has been widely investigated in magnetic materials and disorder is commonly used to generate spin glasses [10]. In general, a spin glass (SG) state prevails in systems dominated by randomness and frustration, which can be realized by either site- or bond-disorder.

Site disorder arises when ions with different magnetic properties may be found randomly distributed on the same crystallographic sites, and is a very effective way to frustrate the Ruderman-Kittel-Kasuya-Yosida (RKKY) interaction. SG alloys such as Cu-Mn, Au-Mn, and Au-Fe belong to this category [11,12]. Moreover, SG can also be induced by diluting magnetic sites using nonmagnetic ions to pass the site-disorder percolation threshold x_s, as in $Eu_{1-x}Sr_xS$ ($x_s \approx 0.136$) [10,13].

Bond disorder arises due to the randomization of bond length. Recent theoretical advances [14,15] strongly suggest that bond disorder is essential to generate a SG state, as realized in transition-metal (TM) pyrochlores (e.g., $Y_2Mo_2O_7$ [2,16–18] and $NaCaCo_2F_7$ [19]) and spinels (e.g., $Zn(Cr_{1-x}Ga_x)_2O_4$ [20–22]). In $Zn(Cr_{1-x}Ga_x)_2O_4$, the SG is not related to the site disorder since the onset composition of SG, $0.2 < x < 0.25$ [22], is well below the percolation threshold of the nonmagnetic Ga^{3+} sites, $x_s \approx 0.61$ [23].

In our opinion, whether bond disorder *alone* can lead to magnetic frustration remains to be seen. Although bond disorder is decisive in $Y_2Mo_2O_7$ and $Zn(Cr_{1-x}Ga_x)_2O_4$ [14,15], its influence on magnetic frustration is not clear due to the coexisting geometric frustration in these materials. Theoretically, it is argued that the weak bond disorder acts as a perturbation to partially lift the degeneracy of a spin liquid [14]. From this point of view, bond disorder does not facilitate magnetic frustration in systems composed of antiferromagnetically coupled spins. In addition, neither of the theories mentioned above could reproduce the critical region ($0.2 < x < 0.25$) for the Néel to SG phase transition in $Zn(Cr_{1-x}Ga_x)_2O_4$ [22].

To demonstrate the exclusive influence of bond disorder on magnetic frustration, or in other words, to avoid geometric frustration, we have studied a series of diluted ferromagnetic TM pyrochlores, $Y_2(M_{1-x}N_x)_2O_7$ (M = magnetic TM ion, N = nonmagnetic ion), where the yttrium sites are nonmagnetic and bond disorder is introduced by the ionic size mismatch between M and N. According to Ref. [23], we expect N sites to percolate at $x_s \approx 0.61$. Specifically, we have employed $Y_2Mn_2^{4+}O_7$ [24] ($x = 0$) as the bond ordered start compound and $Y_2(Cr^{3+}_{1-x}Ga^{3+}_{x-0.5}Sb^{5+}_{0.5})_2O_7$ ($0.5 \leqslant x \leqslant 0.9$) as the bond disordered compounds. The magnetic TM ions in these systems (Mn^{4+} and Cr^{3+}) share the same electronic configuration ($3d^3$). Experimentally, we have performed magnetization and high-resolution neutron powder diffraction (HRNPD) measurements on $Y_2(Cr_{1-x}Ga_{x-0.5}Sb_{0.5})_2O_7$ ($0.5 \leqslant x \leqslant 0.9$). In Y_2CrSbO_7 ($x = 0.5 < x_s$), we find no evidence of zero-field magnetic long-range order down to 1.8 K despite having a

positive Curie-Weiss temperature $\Theta_{CW} \simeq 19.5$ K. Since Cr sites are percolative in Y_2CrSbO_7 [23], site disorder cannot be the driving mechanism of the observed high magnetic frustration. We have also carried out comprehensive numerical simulations to study the percolation processes of various nonmagnetic clusters, including bond disorder, site disorder, and the intermediate types in between (see Sec. III). Based on these simulations, bond disorder percolates at $x_b = 0.23(1)$ on a pyrochlore lattice, pointing to percolative bond disorder in Y_2CrSbO_7 ($x = 0.5$). Our model also explains why the Néel to SG phase transition in $Zn(Cr_{1-x}Ga_x)_2O_4$ happens between $x = 0.2$ and 0.25, as well as the rapid drop in the magnetically ordered moment in the Néel phase upon Ga substitution [22]. The non-negligible role of bond disorder in the zero-field magnetic frustration in Y_2CrSbO_7 is further supported by recovering the magnetic long-range order in a magnetic field ~4 T.

II. EXPERIMENTS

Polycrystalline samples of $Y_2(Cr_{1-x}Ga_{x-0.5}Sb_{0.5})_2O_7$ ($0.5 \leqslant x \leqslant 0.9$) were synthesized by the solid-state reaction method in three steps [25]. First of all, $GaSbO_4$ ($CrSbO_4$) powders were prepared by heating Ga_2O_3 (Cr_2O_3) (3N) and Sb_2O_3 (3N, 5% excess to compensate the volatilization) for 3 days at 640, and then 5 days at 1200 °C with several intermediate regrindings. The intermediate temperature (640 °C) is to transform Sb_2O_3 into Sb_2O_4. To prepare Y_2GaSbO_7 (Y_2CrSbO_7), a stoichiometric mixture (1:1) of $GaSbO_4$ ($CrSbO_4$) and Y_2O_3 (4N) was heated in air for 6 days at 1200 °C with several intermediate regrindings as well. Finally, $Y_2(Cr_{1-x}Ga_{x-0.5}Sb_{0.5})_2O_7$ was obtained by heating the stoichiometrically mixed Y_2GaSbO_7 and Y_2CrSbO_7 powders for 5 days at 1200 °C.

Magnetization data were recorded using a Magnetic Property Measurement System (MPMS, Quantum Design). X-ray powder diffraction measurements were performed using a Bruker D8 diffractometer (Cu Kα1, $\lambda = 1.5406$ Å) at room temperature. HRNPD patterns were collected at the D2B powder diffractometer ($\lambda = 1.594$ Å), equipped with a 5 T vertical cryomagnet, at the Institut Laue-Langevin (ILL) in Grenoble, France [27]. For these measurements, about 8 g of each powder sample were hydraulically pressed into a cylinder (height = 11, diameter = 13 mm) to avoid any field-induced texture and then loaded into a vanadium container. Rietveld refinements were carried out using the FULLPROF package [28].

III. RESULTS AND DISCUSSION

We first discuss the bond ordered compound $Y_2Mn_2O_7$ ($x = 0$). The predominant Mn-Mn exchange is ferromagnetic, as evidenced by $\Theta_{CW} = 41(2)$ K [29]. The effective magnetic moment M_{eff} deduced from fitting the susceptibility vs temperature (χ-T) curve in the paramagnetic region is 3.84(2) μ_B/Mn, indicating $J = S = 3/2$ for Mn^{4+} (J and S are the total and spin angular momenta, respectively) [29]. The orbital quenching in $Y_2Mn_2O_7$ is also confirmed by its saturation moment measured at 5 K: $M_s \approx 3.0\ \mu_B$/Mn [24]. The magnetic ground state of $Y_2Mn_2O_7$ is very sample dependent. Shimakawa *et al.* claim ferromagnetism in their sample based on the λ heat capacity anomaly around 15 K, below which the χ-T curve plateaus [24]. However, the λ anomaly in heat capacity is not observed in the samples prepared by Reimers *et al.* [29] and Greedan *et al.* [30]. Instead, their results strongly support a SG-like state at low temperatures. The strong sample dependence of magnetic properties might be related to the valence disorder in $Y_2Mn_2O_7$, where high pressure synthesis is required to stabilize Mn^{4+} [24,29,31].

While Cr^{4+}-based pyrochlores also require high pressure synthesis [31], Cr^{3+}-based pyrochlores can be prepared at ambient pressure [25]. To avoid the potential complication to the magnetic structure caused by valence disorder, we have chosen to study the Cr^{3+}-based pyrochlore Y_2CrSbO_7, where Sb^{5+} is used to compensate for the valence loss. Cr^{3+} shares the same $3d^3$ electronic configuration as Mn^{4+}. Moreover, the lattice parameters of Y_2CrSbO_7 are analogous to those of $Y_2Mn_2O_7$ (Table I) [26]. As a result, the magnetic interactions in the two systems are expected to be similar.

The field-cooled (FC) and zero-field-cooled (ZFC) χ-T curves of one Y_2CrSbO_7 sample, labeled as S1, are displayed in Fig. 1(a) (inset). The divergence between the ZFC and FC susceptibility around 142 K is related to the onset of the canted antiferromagnetic order in the impurity phase $YCrO_3$ [25]; this phase has a volume fraction of 3.4(2)% in S1, as revealed by our HRNPD measurements [inset of Fig. 1(b)]. A second sample of Y_2CrSbO_7, labeled as S2, was also synthesized; this sample was only characterized by the magnetization technique. The χ-T curves of S2 are only distinct from those of S1 below 142 K. This could be caused by the higher content of $YCrO_3$ in the latter. In order to obtain Θ_{CW} and M_{eff}, we tried to apply the two-population model proposed in Ref. [32] to the data in the paramagnetic region ($146 \leqslant T \leqslant 300$ K). According to this model, the susceptibility can be fitted using the equation

$$\chi = M/H = C^{main}/\left(T - \Theta_{CW}^{main}\right) + C^{imp}/\left(T + \Theta_{CW}^{imp}\right), \quad (1)$$

TABLE I. Structural parameters of $Y_2Mn_2O_7$ (from Ref. [26]), Y_2CrSbO_7, and $Y_2Cr_{0.4}Ga_{0.6}SbO_7$, in which B represents the atomic positions of Mn/Cr/Sb/Ga. The corresponding diffraction patterns were refined under space group *Fd-3m* ($a = b = c$, $\alpha = \beta = \gamma = 90°$). The only atomic position that needs to be refined is O2 (x, 0.125, 0.125).

			B_{iso} (Å^2)						
	a (Å)	x (O2)	Y	B	O1	O2	B-O2 (Å)	B-B (Å)	B-O2-B (°)
$Y_2Mn_2O_7$ (RT)	9.902(1)	0.3274(8)	0.3(1)	0.1(1)	0.1(3)	0.2(1)	1.911(3)	3.5009(3)	132.7(5)
Y_2CrSbO_7 (300 K)	10.1620(1)	0.4178(1)	0.72(1)	0.44(2)	0.15(3)	0.45(1)	1.9810(6)	3.59282(3)	130.14(2)
Y_2CrSbO_7 (2.0 K)	10.1523(7)	0.41793(8)	0.69(1)	0.34(1)	0.17(2)	0.439(8)	1.9787(3)	3.5894(2)	130.19(1)
$Y_2Cr_{0.4}Ga_{0.6}SbO_7$ (2.0 K)	10.1508(8)	0.4182(1)	0.58(1)	0.51(2)	0.17(3)	0.37(1)	1.9774(5)	3.58885(2)	130.31(2)

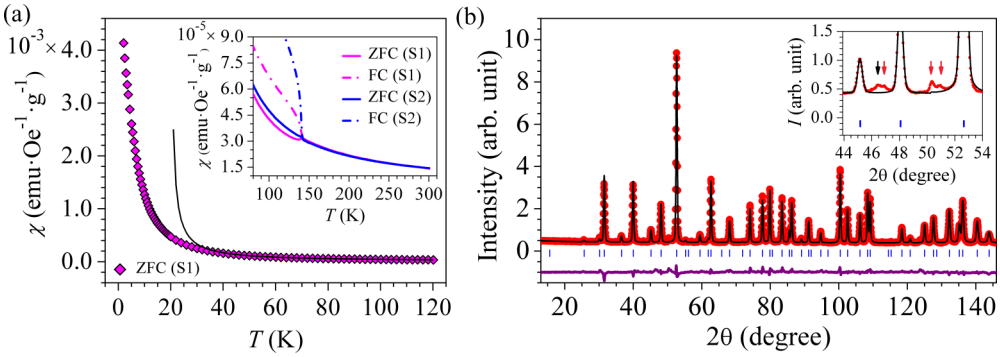

FIG. 1. (a) Main panel: ZFC χ-T curve of Y_2CrSbO_7 (S1) measured at $\mu_0 H = 0.01$ T. The black solid line is a Curie-Weiss fit to the data between 50 and 120 K using Eq. (2). Inset: ZFC and FC χ-T curves of S1 and S2 measured at $\mu_0 H = 0.01$ T. (b) HRNPD pattern (red solids) of Y_2CrSbO_7 (S1) measured at $T = 2.0$ K, and $B = 0$ T. Calculated pattern (black line), nuclear Bragg positions (blue vertical line), and difference (purple line) are also displayed. Inset: Enlarged version of a selected angle region. Additional peaks from $YCrO_3$ (red arrows) and the vanadium sample can (black arrow) can be seen.

where the first and second terms come from the main and impurity phases, respectively. Unfortunately, this method does not work satisfactorily here since the second term in Eq. (1) is too weak to be accurately determined [33]. Instead, we performed Curie-Weiss analysis on both samples between 50 and 120 K. To a good approximation, the magnetization of the minority phase $YCrO_3$ in this region can be treated as a constant [34,35]. Then, the total susceptibility can be written as

$$\chi = M/H = C^{\text{main}}/(T - \Theta_{\text{CW}}) + \chi_{\text{imp}}. \quad (2)$$

This second model has been employed to numerically fit the χ-T curves of $Y_2(Cr_{1-x}Ga_{x-0.5}Sb_{0.5})_2O_7$ between $x = 0.5$ and 0.9; the corresponding parameters are summarized in Table II. The variance in the sign and absolute value of χ_{imp} has been observed in the past; it is related to the large coercive field in $YCrO_3$ [34,35]. Using the volume fraction of $YCrO_3$ in S1, M_{eff} is calculated to be 3.65(2) μ_B/Cr in Y_2CrSbO_7. Moreover, Θ_{CW} extracted from S1 and S2 are identical to each other within the errors; they are also close to the value of 15 K reported in Ref. [36]. These results support ferromagnetic Cr-Cr exchange in this compound. They also indicate that the Weiss molecular fields in Y_2CrSbO_7 and $Y_2Mn_2O_7$ are similar, as Θ_{CW} is proportional to the number of magnetic sites per unit cell × the Weiss molecular field [37]. Our fitting also reveals that C^{main} decreases monotonously upon Ga substitution (Table II). This is expected because C^{main} is proportional to the number of magnetic sites per unit cell [37]. Unlike C^{main}, Θ_{CW} does not show a clear substitution dependence; this could be related to the concomitant change in the Weiss molecular field.

TABLE II. The fitted parameters in Eq. (2) at different compositions x of $Y_2(Cr_{1-x}Ga_{x-0.5}Sb_{0.5})_2O_7$.

x	C^{main} (emu · K / Oe · g)	Θ_{CW} (K)	χ_{imp} (emu / Oe · g)
0.5	S1: $3.48(5) \times 10^{-3}$	S1: 19.6(4)	S1: $-0.6(3) \times 10^{-6}$
	S2: $3.68(1) \times 10^{-3}$	S2: 19.2(1)	S2: $1.91(1) \times 10^{-6}$
0.6	$3.20(3) \times 10^{-3}$	13.6(4)	$-1.8(2) \times 10^{-6}$
0.7	$2.36(3) \times 10^{-3}$	14.9(5)	$-1.2(2) \times 10^{-6}$
0.8	$1.72(2) \times 10^{-3}$	13.0(5)	$-1.2(1) \times 10^{-6}$
0.9	$0.93(2) \times 10^{-3}$	11.6(7)	$-1.4(1) \times 10^{-6}$

Deviation from paramagnetism can be observed in Y_2CrSbO_7 below 50 K, as revealed by the Curie-Weiss fit to the ZFC χ-T curve [main panel of Fig. 1(a)]. Surprisingly, no ferromagnetism can be observed down to 1.8 K for Y_2CrSbO_7. The absence of magnetic long-range order in Y_2CrSbO_7 is further confirmed by our HRNPD measurements at 2 K; only crystallographic reflections can be resolved in the recorded diffraction pattern [Fig. 1(b)]. These observations are in agreement with earlier work [36].

Within the resolution of our Rietveld refinement (∼1%), the Cr:Sb ratio is 1:1 in Y_2CrSbO_7. Based on Ref. [23], nonmagnetic sites percolate at $x_s \approx 0.61$ on a pyrochlore lattice. Thus, the Cr sites in Y_2CrSbO_7 ($x = 0.5$) are still percolative with a fraction $f_M = 83(2)\%$ [see Fig. 2(c) obtained from our simulations, details of which will be discussed below]. For a ferromagnetic TM pyrochlore, magnetic frustration is often negligible due to the lack of possible sources. The expected ferromagnetically ordered moment M_{exp} in Y_2CrSbO_7 can be estimated to be $0.83(2)gJ \sim 2.31(6)\ \mu_B$/Cr, where the Landé g factor is approximately 2 and $J = 1.39(1)$ is extracted from M_{eff}. M_{exp} is well above the resolution of our HRNPD measurements (<0.5 μ_B). The magnetic frustration in Y_2CrSbO_7 is reflected by the frustration index, $h = |\frac{\Theta_{\text{CW}}}{T_t}| > 10$, where T_t is the transition temperature. h is 2.7 in $Y_2Mn_2O_7$ and close to 1 in nonfrustrated magnets. This high level of frustration is not usually expected for ferromagnetically coupled spins [38]. One possible origin for the suppressed T_t in Y_2CrSbO_7 is nonmagnetic site disorder. The critical concentration where the magnetic long-range order disappears is very close, if not equal, to $x_s \approx 0.61$ [39–42], meaning conventional ferromagnetism should still develop in Y_2CrSbO_7 ($x = 0.5$) below 1.8 K. However, the χ-T curves in the high field region do not support this scenario (Fig. 3). These magnetic fields are expected to smooth out the ferromagnetic phase transition and leave T_t unchanged [37].

When diluting the magnetic sites by nonmagnetic ions, bond disorder is also introduced to the local lattice due to the inevitable ionic size mismatch between M and N. As a result,

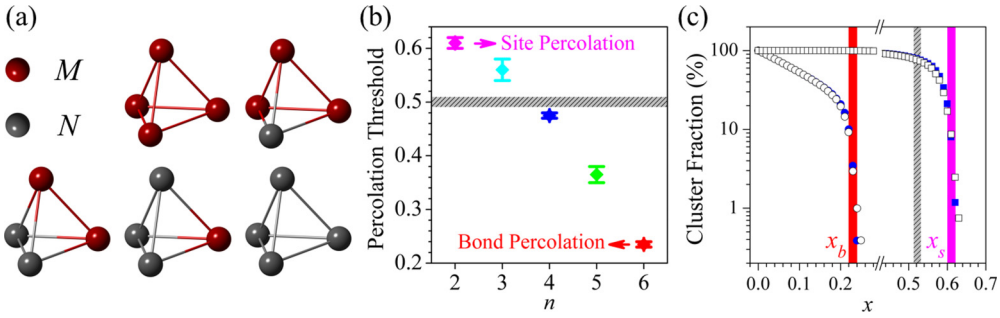

FIG. 2. (a) Five possible configurations of an M/N-tetrahedron. (b) The percolation thresholds produced by our simulations on a $D \times D \times D$ pyrochlore lattice with s sampling times of bond disorder (red, $D = 64$ and $s = 100$); Cr clusters with at least five (green, $D = 64$ and $s = 16$), four (blue, $D = 48$ and $s = 16$), and three (cyan, $D = 48$ and $s = 16$) nearest neighbor Cr sites; and site disorder (magenta, $D = 64$ and $s = 50$). (c) The evolution of the fraction of percolative bond- (circles) and site- (squares) ordered clusters as a function of the nonmagnetic fraction x (blue closed: $D = 48$, black open: $D = 64$). The red (magenta) area marks the percolation region of bond (site) disorder. The gray hatched areas in (b) and (c) mark the position of Y_2CrSbO_7 with $\Delta x = 0.01$.

there will be five types of M/N-tetrahedra in $Y_2(M_{1-x}N_x)_2O_7$, which can be labeled as empty, single, double, triple, and full in terms of M occupation [Fig. 2(a)]. For site percolation, bond disorder is ignored so that the percolation of doubly, triply, and fully occupied tetrahedra are calculated simultaneously. For the bond percolation, on the other hand, bond disorder is the focus. Bond disorder will randomly distort the local TMO_6 octahedron, frustrating the crystal field. Moreover, the random distribution of M-O-M bond angles caused by bond disorder will lead to exchange fluctuations. Similar effects have been intensively studied in the SG pyrochlore $Y_2Mo_2O_7$, where the Mo-Mo exchange is antiferromagnetic and bond disorder comes from orbital frustration [14,15,43,44].

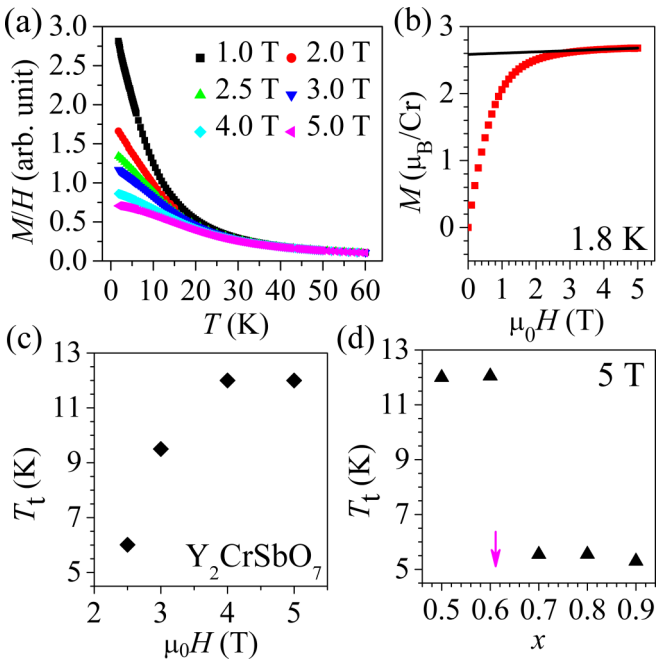

FIG. 3. (a) Susceptibility (M/H) of Y_2CrSbO_7 (S1) vs temperature curves in the high field region. (b) Field scan of the magnetization of Y_2CrSbO_7 at 1.8 K. The black line is a linear fit to the data above 3.5 T. (c) Magnetic field dependence of the transition temperature T_t in Y_2CrSbO_7. (d) x dependence of T_t measured at 5 T, showing the recovery of site percolation. The vertical arrow marks the position of x_s.

To qualitatively elucidate the effect of bond disorder, we have simulated the percolation processes of Cr sites with at least two (site percolation), three, four, five, and six (bond percolation) nearest neighbor Cr sites, respectively. The simulations were performed on a $D \times D \times D$ ($D = 48$, 64) cubic pyrochlore lattice (corner-sharing tetrahedral network). This lattice, initially with all sites occupied by magnetic ions ($x = 0$), was randomly diluted by nonmagnetic ions to the required composition x. For each composition, the percolation probability is 1 if at least one percolative path is found between any of the two parallel facets of the cube in our simulations. The simulations for each x were sampled by s times. As shown in Fig. 2(b), the site percolation threshold, $x_s = 0.61(1)$, produced by our simulations is consistent with the previous study [23]. In addition, our simulations also predict that bond percolation occurs well ahead of site percolation at $x_b = 0.23(1)$ [Fig. 2(b)]. Due to the valence constraint, we are unable to check x_b in our samples, $Y_2(Cr_{1-x}Ga_{x-0.5}Sb_{0.5})_2O_7$ ($0.5 \leqslant x \leqslant 0.9$). However, we have identified a spinel system, $Zn(Cr_{1-x}Ga_x)_2O_4$, where the Cr/Ga sites form a pyrochlore sublattice. The clean compound $ZnCr_2O_4$ ($x = 0$) undergoes a spin-Peierls-like phase transition at $T_N = 12.5$ K [45]. By increasing the nonmagnetic Ga fraction x on Cr sites, the magnetically ordered moment drops rapidly to zero; a Néel to SG transition sets in between 0.2 and 0.25 [22]. These results are in excellent agreement with our bond percolation model (Fig. 2). The transition temperatures of both Néel order and SG decrease monotonously as a function of x in $Zn(Cr_{1-x}Ga_x)_2O_4$ [22]. Theoretically, bond disorder is responsible for the onset of the SG state in $Zn(Cr_{1-x}Ga_x)_2O_4$ [14,15]. As a result, we propose that Y_2CrSbO_7 might also undergo a spin-freezing transition at very low temperatures (<1.8 K), forming a SG magnetic ground state.

In addition to bond disorder, a pyrochlore lattice might be transformed into a hyperkagome lattice by nonmagnetic-ion dilution, which imposes a new geometric frustration effect on the spin lattice. A hyperkagome lattice is composed of a three-dimensional corner-sharing triangular network, which can be realized by selectively removing one of the four sites

in each tetrahedron of a pyrochlore lattice [46,47]. Since it is a special case of nonmagnetic-ion dilution, we have performed separate simulations on this problem, from which we find that random substitution does not induce a percolative hyperkagome lattice in the entire region. On the other hand, local hyperkagome clusters do exist on a diluted pyrochlore lattice. The fraction of these clusters, f, can be exactly calculated using

$$f = (1-x)\left\{\frac{3x(1-x)^2}{(1-x)^3+3x(1-x)^2+3x^2(1-x)+x^3}\right\}^2. \quad (3)$$

In Y_2CrSbO_7 ($x = 0.5$), $f \simeq 7\,\%$. Due to the local feature of the hyperkagome lattice and the small fraction of these clusters, we conclude that the hyperkagome lattice is not the decisive force to the magnetic ground state of the majority spins in Y_2CrSbO_7.

The ionic radii of Cr^{3+}, Ga^{3+}, and Sb^{5+} are 0.615, 0.62, and 0.60 Å, respectively [48]. As a result, the strength of bond disorder in this system is very weak, but still sufficient to see an effect. Advanced SG theories, which can be applied to $Zn(Cr_{1-x}Ga_x)_2O_4$ and $Y_2Mo_2O_7$, have demonstrated a spin freezing transition in the zero bond-disorder limit. To estimate the strength of bond disorder in $Y_2(Cr_{1-x}Ga_{x-0.5}Sb_{0.5})_2O_7$, we examine the magnetic properties under an external perturbation, i.e., magnetic field. As shown in Fig. 3(a), a low temperature magnetization plateau gradually develops in Y_2CrSbO_7 as the magnetic field is increased. The field dependence of the magnetization is displayed in Fig. 3(b). The magnetization is saturated between 3.0 and 4.0 T with $M_s = 2.59\ \mu_B$/Cr. M_s is between M_{exp} and $gJ = 2.78(2)\ \mu_B$/Cr. This may suggest that only the spins on percolative Cr sites are ordered. The transition temperature T_t is defined as the point where the corresponding χ-T curve has the steepest slope. The continuous increase of T_t as a function of magnetic field ($\mu_0 H < 4$ T) supports the idea of a highly frustrated zero-field magnetic ground state with nonuniform bond disorder. At 4 T and above, T_t of Y_2CrSbO_7 tends to saturate at ~12 K [Fig. 3(c)]. This deviates from the behavior of a polarized paramagnet [37]. We note that T_t only saturates when the percolative Cr spins are fully aligned. In other words, magnetic long-range order is fully recovered in Y_2CrSbO_7 when the magnetic frustration is removed. As a result, the strength of bond disorder in Y_2CrSbO_7 is estimated to range from 0 to 3.5 T. A sudden drop in T_t measured at 5 T is observed between 0.6 and 0.7 [Fig. 3(d)]. It means that long-range spin correlation, which is recovered by suppressing the magnetic frustration caused by bond disorder, develops in the high field region for $x < x_s = 0.61(1)$. It also indicates that our samples are stoichiometrically homogeneous with $\Delta x < 0.02$.

IV. SUMMARY

Based on our magnetization and HRNPD measurements (Fig. 1), we have observed a very high level of magnetic frustration ($h > 10$) in the TM pyrochlore Y_2CrSbO_7 where the Cr-Cr exchange is predominantly ferromagnetic. The magnetic frustration cannot be explained by nonmagnetic site disorder (Sb). We propose percolative bond disorder caused by the ionic size mismatch as the driving mechanism. The average Cr/Sb-O-Cr/Sb bond angle is 130.19(1)° in Y_2CrSbO_7. Based on a previous study on the Cr-based oxides with very similar lattice parameters, this value is in the critical region where the Cr-Cr exchange interaction changes its sign [49]. Because of this, zero point exchange fluctuations might be present although the overall exchange is ferromagnetic. Secondly, bond disorder will also affect the local crystal field environment, e.g., frustrating the single-ion anisotropy. We have also estimated the strength of bond disorder in Y_2CrSbO_7, which is in the region of [0 T, 3.5 T]. As a result, both magnetic long-range order and site percolation process can be recovered by applying high magnetic fields (Fig. 3).

For $Y_2(M_{1-x}N_x)_2O_7$ (M = magnetic TM ion, N = nonmagnetic ion), we have performed numerical simulations to study the percolation process of various clusters, including bond disorder, site disorder, and several intermediate states in between. Our results unambiguously reveal that bond disorder [$x_b = 0.23(1)$] percolates well ahead of site disorder [$x_s = 0.61(1)$]. More importantly, our model can be experimentally verified in the spinel system $Zn(Cr_{1-x}Ga_x)_2O_4$ where a Néel to SG transition can be induced by Ga substitution (Fig. 2) [22]. Considering the similarity between the Cr/Sb- and Cr/Ga-sublattices in many aspects, we propose that the magnetic ground state of Y_2CrSbO_7 is a SG. We also call for further investigations in the future. For example, experiments, e.g., heat capacity and HRNPD, in the ultralow temperature region (<1.8 K) would be helpful to understand the magnetic ground state of Y_2CrSbO_7. Investigations on the local crystallographic structure are needed to check the amplitude of exchange fluctuations.

ACKNOWLEDGMENTS

We thank M. W. Long and E. M. Forgan for helpful discussions. We acknowledge the U.K. Engineering and Physical Sciences Research Council for funding under Grant No. EP/J016977/1.

[1] H. T. Diep, *Frustrated Spin Systems*, 2nd ed. (World Scientific, Singapore, 2013).
[2] J. S. Gardner, M. J. P. Gingras, and J. E. Greedan, Rev. Mod. Phys. **82**, 53 (2010).
[3] R. Moessner and J. T. Chalker, Phys. Rev. Lett. **80**, 2929 (1998).
[4] R. Moessner and J. T. Chalker, Phys. Rev. B **58**, 12049 (1998).
[5] B. Canals and C. Lacroix, Phys. Rev. Lett. **80**, 2933 (1998).
[6] M. J. Harris, S. T. Bramwell, D. F. McMorrow, T. Zeiske, and K. W. Godfrey, Phys. Rev. Lett. **79**, 2554 (1997).
[7] S. T. Bramwell and M. J. P. Gingras, Science **294**, 1495 (2001).
[8] D. J. P. Morris, D. A. Tennant, S. A. Grigera, B. Klemke, C. Castelnovo, R. Moessner, C. Czternasty, M. Meissner, K. C. Rule, J.-U. Hoffmann, K. Kiefer, S. Gerischer, D. Slobinsky, and R. S. Perry, Science **326**, 411 (2009).

[9] C. Castelnovo, R. Moessner, and S. L. Sondhi, Nature (London) **451**, 42 (2008).
[10] K. Binder and A. P. Young, Rev. Mod. Phys. **58**, 801 (1986).
[11] S. Nagata, P. H. Keesom, and H. R. Harrison, Phys. Rev. B **19**, 1633 (1979).
[12] A. F. J. Morgownik and J. A. Mydosh, Solid State Commun. **47**, 321 (1983).
[13] H. Maletta and W. Felsch, Phys. Rev. B **20**, 1245 (1979).
[14] T. E. Saunders and J. T. Chalker, Phys. Rev. Lett. **98**, 157201 (2007).
[15] H. Shinaoka, Y. Tomita, and Y. Motome, Phys. Rev. Lett. **107**, 047204 (2011).
[16] M. J. P. Gingras, C. V. Stager, N. P. Raju, B. D. Gaulin, and J. E. Greedan, Phys. Rev. Lett. **78**, 947 (1997).
[17] K. Miyoshi, Y. Nishimura, K. Honda, K. Fujiwara, and J. Takeuchi, J. Phys. Soc. Jpn. **69**, 3517 (2000).
[18] J. E. Greedan, M. Sato, X. Yan, and F. S. Razavi, Solid State Commun. **59**, 895 (1986).
[19] R. Sarkar *et al.*, arXiv:1604.00814.
[20] W. Ratcliff, S.-H. Lee, C. Broholm, S.-W. Cheong, and Q. Huang, Phys. Rev. B **65**, 220406 (2002).
[21] D. Fiorani, S. Viticoli, J. L. Dormann, J. L. Tholence, and A. P. Murani, Phys. Rev. B **30**, 2776 (1984).
[22] S.-H. Lee, W. Ratcliff, Q. Huang, T. H. Kim, and S.-W. Cheong, Phys. Rev. B **77**, 014405 (2008).
[23] C. L. Henley, Can. J. Phys. **79**, 1307 (2001).
[24] Y. Shimakawa, Y. Kubo, N. Hamada, J. D. Jorgensen, Z. Hu, S. Short, M. Nohara, and H. Takagi, Phys. Rev. B **59**, 1249 (1999).
[25] M. J. Whitaker and C. Greaves, J. Solid State Chem. **215**, 171 (2014).
[26] M. Subramanian, C. Torardi, D. Johnson, J. Pannetier, and A. Sleight, J. Solid State Chem. **72**, 24 (1988).
[27] L. Shen, E. Blackburn, T. Hansen, and R. Riyat, Institut Laue-Langevin (ILL), (2014), doi:10.5291/ILL-DATA.5-31-2332.
[28] J. Rodríguez-Carvajal, Physica B (Amsterdam) **192**, 55 (1993).
[29] J. N. Reimers, J. E. Greedan, R. K. Kremer, E. Gmelin, and M. A. Subramanian, Phys. Rev. B **43**, 3387 (1991).
[30] J. E. Greedan, N. P. Raju, A. Maignan, C. Simon, J. S. Pedersen, A. M. Niraimathi, E. Gmelin, and M. A. Subramanian, Phys. Rev. B **54**, 7189 (1996).
[31] H. Fujinaka, N. Kinomura, M. Koizumi, Y. Miyamoto, and S. Kume, Mater. Res. Bull. **14**, 1133 (1979).
[32] P. Schiffer and I. Daruka, Phys. Rev. B **56**, 13712 (1997).
[33] According to Ref. [36] and our analysis, Θ_{CW} is between 15 and 20 K in Y_2CrSbO_7. On the other hand, Θ_{CW} is around 450 K in $YCrO_3$. Moreover, C^{imp} is much smaller than C^{main} due to the minor fraction of $YCrO_3$ [Eq. (1)] [37]. As a result, the second term in Eq. (1) is very small. We have tried to forcibly fit the data using Eq. (1). Although $C^{main} = 3.7(1) \times 10^{-6}$ emu·K/Oe and $\Theta_{CW}^{main} = 20(2)$ K agree with the values extracted by Eq. (2), enormously large errors are obtained for C^{imp} and Θ_{CW}^{imp}.
[34] G. N. P. Oliveira, P. Machado, A. L. Pires, A. M. Pereira, J. P. Araújo, and A. M. L. Lopes, J. Phys. Chem. Solids **91**, 182 (2016).
[35] Y. Sharma, S. Sahoo, W. Perez, S. Mukherjee, R. Gupta, A. Garg, R. Chatterjee, and R. S. Katiyar, J. Appl. Phys. **115**, 183907 (2014).
[36] P. F. Bongers and E. R. V. Meurs, J. Appl. Phys. **38**, 944 (1967).
[37] S. Blundell, *Magnetism in Condensed Matter* (Oxford University Press, Oxford, 2011).
[38] We note that the frustration index h may not accurately describe the level of frustration in magnetic solids. For example, in the perovskite manganites there is strong random frustration caused by the interplay between spin, charge, orbital, and lattice degrees of freedom, e.g., see Dagotto *et al.*, Phys. Rep. **344**, 1 (2001), but h is not impressively high in these materials. In addition to magnetic frustration, the transition temperature can also be suppressed by reduced dimensionality and quantum fluctuations, leading to a high value of h, e.g., see Li *et al.*, Phys. Rev. Lett. **115**, 167203 (2015). However, these two factors are not relevant in Y_2CrSbO_7, as it crystallizes into a three-dimensional pyrochlore lattice and possesses an effective spin of $S = 3/2$ per Cr. We consider that the high h in Y_2CrSbO_7 exclusively results from the bond-disorder induced magnetic frustration discussed in the main text.
[39] S.-W. Cheong, A. S. Cooper, L. W. Rupp, B. Batlogg, J. D. Thompson, and Z. Fisk, Phys. Rev. B **44**, 9739 (1991).
[40] D. J. Breed, K. Gilijamse, J. W. E. Sterkenburg, and A. R. Miedema, J. Appl. Phys. **41**, 1267 (1970).
[41] D. Kumar and A. B. Harris, Phys. Rev. B **8**, 2166 (1973).
[42] R. A. Tahir-Kheli, T. Fujiwara, and R. J. Elliott, J. Phys. C **11**, 497 (1978).
[43] J. A. Paddison *et al.*, arXiv:1506.05045.
[44] J. E. Greedan, D. Gout, A. D. Lozano-Gorrin, S. Derahkshan, T. Proffen, H.-J. Kim, E. Božin, and S. J. L. Billinge, Phys. Rev. B **79**, 014427 (2009).
[45] S.-H. Lee, C. Broholm, T. H. Kim, W. Ratcliff, and S.-W. Cheong, Phys. Rev. Lett. **84**, 3718 (2000).
[46] Y. Okamoto, M. Nohara, H. Aruga-Katori, and H. Takagi, Phys. Rev. Lett. **99**, 137207 (2007).
[47] M. J. Lawler, H.-Y. Kee, Y. B. Kim, and A. Vishwanath, Phys. Rev. Lett. **100**, 227201 (2008).
[48] R. D. Shannon, Acta Crystallogr. Sect. A **32**, 751 (1976).
[49] K. Motida and S. Miyahara, J. Phys. Soc. Jpn. **28**, 1188 (1970).